EurJOC
European Journal of Organic Chemistry

DOI: 10.1002/ejoc.201300641

Oxazolone-Based Photoswitches: Synthesis and Properties

Marina Blanco-Lomas,[a] Ignacio Funes-Ardoiz,[a] Pedro J. Campos,[a] and Diego Sampedro*[a]

Keywords: Photochemistry / Molecular devices / Photoswitches / Density functional calculations / Heterocycles

The synthesis, photophysics and photochemistry of a family of molecular switches inspired by the green fluorescent protein (GFP) chromophore is presented. These compounds can be synthesized in one step and good yields, their photophysical properties may be tuned by the substituents, solvent and wavelength of irradiation, and they show very efficient and fast photoisomerization. Furthermore, their high thermal stability and limited photodecomposition could allow these switches to be used in a range of applications. Finally, oxazolone photoswitches may be activated by the use of light and deactivated by either heat or light of a different wavelength.

Introduction

In recent years, the convergence of many different scientific disciplines has led to the design and study of a number of synthetic molecular devices that have been inspired, in some cases, by biomolecular machines acting inside living cells. Diverse types of molecular devices and machines have been developed, but it is probably the field of molecular switches that has been most widely studied. As a general definition, a molecular switch is a bistable system in which each state can be converted into the other by the effect of an external stimulus.[1] Although many different types of molecular switches have been reported, two main families are clearly recognized; switches acting through the isomerization of a double bond and through a cyclization process. Among the switches based on isomerization, azobenzenes, overcrowded alkenes, and retinal-based switches are the most popular.[2] Regarding the second type, fulgides,[3] diarylethenes,[4] spiropyran compounds,[5] and dihydroazulenes have been used as molecular switches involving a photocyclization process.[6] In both cases, light energy is a convenient stimulus with several practical advantages.[7] The use of many of these photoswitches in different contexts has allowed the development of interesting applications in fields such as the control of wettability in polymers,[8] color modification in liquid crystals,[9] and reversible photocontrol of peptide conformations,[10] to mention some examples. Most of the applications of photoswitches developed to date involve the use of azobenzenes, and this type of compound is the best known photoswitch. However, the use of switches in complex systems is usually hampered by the relatively low number of systems capable of performing efficient photoisomerization under different requisites of solubility, wavelength of use, photostationary state and thermal stability.

We have recently reported[11a] a new family of compounds based on the green fluorescent protein (GFP; Scheme 1) that are capable of efficient photoswitching behavior. The green fluorescent protein was first obtained from *Aequorea victoria* jellyfish and was the first example of intrinsically fluorescent molecules with optical properties determined by a photoexcitable green-light emitter chromophore.[12] Beyond its emitting properties, several studies have shown that the GFP chromophore may also undergo other nonradiative processes, such as *Z*/*E* photoisomerization. Although this contributes to reducing the luminescence quantum yield,[13] it also permits the photophysical and photochemical properties of the chromophore to be tuned through modifications of the imidazoline GFP moiety. Accordingly, several modified GFPs have been reported to show relevant photophysical and photochemical processes.[13b,14] Oxazolone derivatives have been extensively used as intermediates in the synthesis of GFP derivatives, but their photophysical and photochemical properties have rarely been explored,[15] even though their photoisomerization has long been known.[16]

Results and Discussion

Synthesis

Using classical conditions for the formation of azalactones,[17] we were able to synthesize a range of compounds with structures based on the GFP chromophore

---

[a] Departamento de Química, Centro de Investigación en Síntesis Química (CISQ), Universidad de La Rioja,
Madre de Dios 51, 26006 Logroño, La Rioja, Spain
E-mail: diego.sampedro@unirioja.es
http://cisq.unirioja.es/grufor.php

Supporting information for this article is available on the WWW under http://dx.doi.org/10.1002/ejoc.201300641.

(Scheme 1). The main difference between the GFP chromophore and the oxazolone analogues is the presence of an amide function in the five-membered ring (dihydroimidazolone) in the GFP chromophore rather than the ester function [5(4*H*)-oxazolones]. We were able to prepare a number of derivatives with different substitution patterns by using this methodology (Table 1). Interestingly, in all cases, only the *Z* isomer was detected in the crude reaction mixture. However, the use of certain benzaldehyde derivatives, such as 2-carboxybenzaldehyde or 2-cyanobenzaldehyde, and most ketones (i.e., acetophenone, benzophenone, 2-hexanone, 1-indanone, 9-oxo-9*H*-fluorene-4-carboxylic acid and methyl 9-oxo-9*H*-fluorene-4-carboxylate), did not lead to the final product. The configuration assignment was made on the basis of X-ray diffraction data for several compounds.[11]

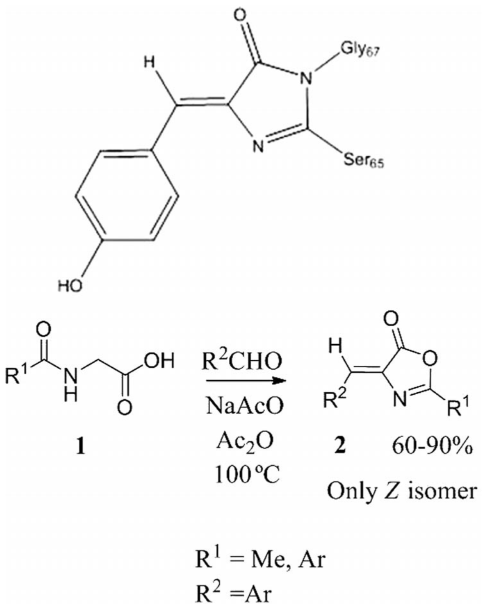

Scheme 1. GFP chromophore (top) and synthesis for GFP-based photoswitches **2**.

Table 1. Synthesized molecular photoswitches.

Entry	R^1	R^2	Compd.	Yield
1	Ph	Ph	**2a**	85%
2	Ph	*p*-Tol	**2b**	85%
3	Ph	*p*-MeOPh	**2c**	60%
4	Ph	*o*-MeOPh	**2d**	87%
5	Ph	*p*-BrPh	**2e**	72%
6	Ph	*o*-BrPh	**2f**	85%
7	Ph	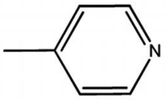	**2g**	[a]
8	Me	Ph	**2h**	80%
9	Me	*p*-Tol	**2i**	75%
10	Me	*p*-MeOPh	**2j**	65%
11	Me	*o*-MeOPh	**2k**	82%
12	Me	*p*-NO$_2$Ph	**2l**	90%
13	Me	*p*-CNPh	**2m**	80%
14	Me	*p*-CO$_2$MePh	**2n**	60%
15	Me	*p*-BrPh	**2o**	72%
16	Me	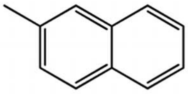	**2p**	61%
17	Me	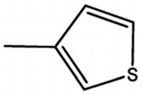	**2q**	74%
18	Me	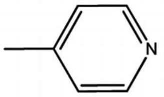	**2r**	[a]
19	*p*-Tol	*p*-Tol	**2s**	80%
20	Me	*o*-Br	**2t**	42%
21	Ph	*p*-NO$_2$Ph	**2u**	71%
22	Ph	*p*-CN	**2v**	34%

[a] Could not be recrystallized from the crude material.

To test the applicability of these compounds in different contexts, a study of the stability of products **2** in diverse solvents was undertaken. It had previously been reported by Herbst et al. that related compounds undergo a hydrolysis reaction in boiling water and acetone for 4 h.[18] Thus, samples of **2h** were dissolved in several flasks with different solvents, such as dichloromethane, acetonitrile, methanol, and aqueous sodium hydroxide (1 M solution; **2h** was not soluble in water). All the solutions were stirred at room temperature for two weeks. In the flasks with dichloromethane and acetonitrile, **2h** was recovered unchanged. However, in flasks containing methanol and sodium hydroxide, a new product was found instead of the starting compound **2h**. In the case of aqueous sodium hydroxide solution, hydrolysis of **2h** to give the corresponding open acetylamino acid occurred. Alternatively, when methanol was used as the solvent, the acetamidoacetate derivative was identified on the basis of MS (ESI$^+$), and ^{1}H and ^{13}C NMR spectroscopic data. Thus, it was concluded that these compounds are stable in non-nucleophilic solvents and only moderately stable in the presence of nucleophiles, which should be taken into account when designing applications in complex systems for these compounds.

UV/Vis Spectra

Prior to the irradiation process, the UV/Vis spectra for all the synthesized compounds were measured. The values for the maximum wavelengths and the extinction coefficients of the bands found for each compound in acetonitrile are presented in Table 2. We can conclude that a bathochromic shift of the maximum wavelength of absorption takes place when R^1 is changed from a methyl (**2i**; entry 8) to a phenyl (**2b**; entry 2) group due to the extended conjugation. A redshift also occurs when R^1 = Me and R^2 varies from Ph (**2h**; entry 7) to *p*-MeOPh (**2j**; entry 9), *p*-NO_2Ph (**2l**; entry 11), or 3-thiophene (**2q**; entry 16). Finally, it should be highlighted that compounds with R^1 = Ph (**2c** and **2d**) present absorption in the visible region (see UV/Vis spectrum of **2c**, Figure 1). Depending on the applications, this is a relevant feature in an efficient photoswitch, because, in this case, low-energy light could be used; this is a required condition in biological media in which more energetic light could damage the system.

Table 2. UV/Vis spectra for molecular photoswitches **2**.

Entry	R^1	R^2	Compd.	λ_{max} (nm)/ε ($M^{-1}cm^{-1}$) in CH_3CN
1	Ph	Ph	**2a**	360 / 81673
2	Ph	*p*-Tol	**2b**	367 / 33333
3	Ph	*p*-MeOPh	**2c**	381 / 37436 403 / 32821
4	Ph	*o*-MeOPh	**2d**	385 / 12394 403 / 10704
5	Ph	*p*-BrPh	**2e**	366 / 37839
6	Ph	*o*-BrPh	**2f**	366 / 10492
7	Me	Ph	**2h**	327 / 26633
8	Me	*p*-Tol	**2i**	336 / 39091
9	Me	*p*-MeOPh	**2j**	355 / 28261
10	Me	*o*-MeOPh	**2k**	363 / 27900
11	Me	*p*-NO_2Ph	**2l**	350 / 24769
12	Me	*p*-CNPh	**2m**	334 / 39000
13	Me	*p*-CO_2MePh	**2n**	331 / 20909
14	Me	*p*-BrPh	**2o**	333 / 24407
15	Me	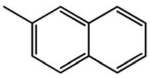	**2p**	342 / 25490
16	Me	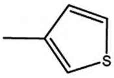	**2q**	358 / 20679
17	*p*-Tol	*p*-Tol	**2s**	370 / 37273
18	Me	*o*-Br	**2t**	330 / 18857
19	Ph	*p*-NO_2Ph	**2u**	376 / 47450
20	Ph	*p*-CN	**2v**	370 / 45960

The UV/Vis spectra of the compounds shown in Table 2 were measured in diverse solvents with different polarity,[19] acetonitrile (polarity 0.460) and chloroform (polarity 0.259), to establish whether there was any solvent effect. It was found that the maximum absorption wavelength of the band undergoes a slight redshift when changing from a polar (acetonitrile) to a less polar (chloroform) solvent. However, in general terms, it can be concluded that the UV spectrum does not change significantly with the solvent.

Irradiation

From the analysis of the UV/Vis spectra it can be concluded that for irradiating the different compounds, a Pyrex filter can be used to avoid radiation below 290 nm (see Figure 1). Thus, a 125 W medium-pressure Hg lamp was used as light source. The results obtained upon irradiation of 0.01 м solutions of several compounds in acetonitrile in an immersion well reactor are shown in Table 3. The photoisomerization process was followed by ^{1}H NMR spectroscopic analysis at time intervals until a photostationary state (PSS) was reached. Integration of the ^{1}H NMR signals corresponding to each isomer provided the isomeric ratio at a given irradiation time. Depending on the photoswitch **2**, the irradiation took from 1 to 3 h to reach the PSS.

Some conclusions could be drawn from the data shown in Table 3. When changing R^1 from methyl (**2h**; entry 5) to phenyl (**2a**; entry 1), little noticeable change of the isomer ratio at the PSS was observed. However, the values for the isomer ratio at the PSS did depend on the substituents on the phenyl group in R^2. Thus, when R^1 was kept constant (Ph) and the substituent on the phenyl group in R^2 was changed from a *para* (**2c**; entry 2) to an *ortho* (**2d**; entry 3) methoxy group, it was observed that the percentage of the *E* isomer increased. There was also an increase of the percentage of *E* isomer present at the PSS when maintaining R^1 = Me and changing R^2 from a phenyl (**2h**; entry 5) to a heterocycle such as 3-thiophene (**2q**; entry 14). Finally, the *E*-isomer could be obtained as the main isomer in the PSS in the case of **2v**. Therefore, it can be seen that the isomer ratio at the PSS can be controlled by the structure.

The two isomers (*Z* and *E*) produced after irradiation could be purified by flash chromatography on silica gel (hexane/ethyl acetate, 10:1) and individually characterized. The isolated *Z* and *E* isomers could then be used to study the kinetics of the isomerization reaction. For this purpose, in two Pyrex NMR tubes, solutions of *E*- and *Z*-**2k** of the same concentration were prepared in $CDCl_3$. The isomer ratio extracted from the ^{1}H NMR spectra were then plotted against irradiation time (Figure 2) for samples with 100% *Z*-**2k** or *E*-**2k** isomer at the beginning of the reaction (t_{irrad} = 0 min). From the linear relationship of $\ln[A_0]/[A]$ vs. irradiation time for the first points of each graph of Figure 2, the kinetic constant of each process was calculated and, thus, the value of the relative kinetic constant that relates the speed of both processes was determined. In this particular case, if $k_{Z\rightarrow E} = 1$, then $k_{E\rightarrow Z} \approx 3$, which means that the

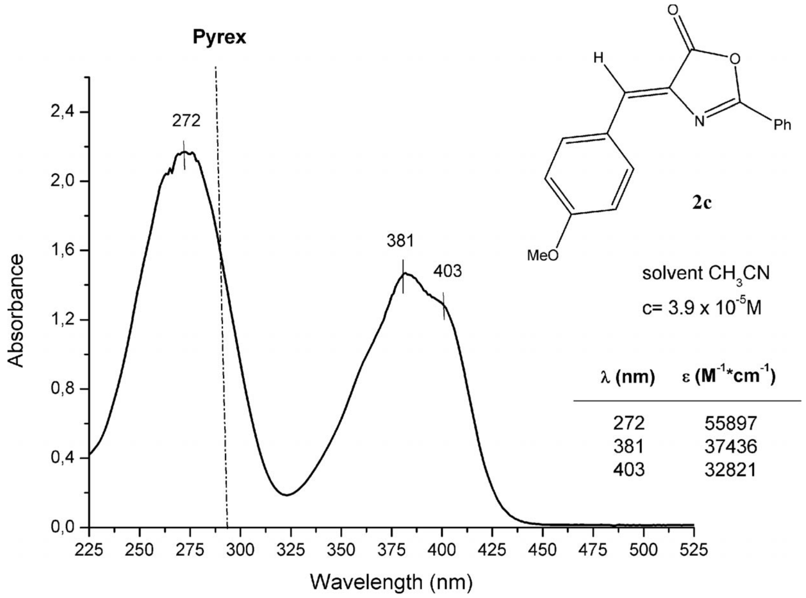

λ (nm)	ε (M^{-1}*cm^{-1})
272	55897
381	37436
403	32821

Figure 1. UV/Vis absorption spectrum of *Z*-**2c** in acetonitrile.

E→*Z* isomerization process is three times faster than the *Z*→*E* reaction. The values of the isomerization quantum yield have only been calculated for the *Z*→*E* and the *E*→*Z* processes of compound **2h**. These values have been previously reported.[11a]

The isomer ratio remained unchanged upon heating for several hours (50 °C in the dark), samples that had previously reached the PSS. Only when samples were heated in refluxing toluene did the mixture slowly revert to the thermodynamically more stable *Z* isomer. These results imply a fast photoisomerization and a high thermal stability, which is quite general for this family of compound.[11]

To gain deeper insight into the factors that control the photoisomerization, we then undertook detailed study of the photophysics and photochemistry of the oxazolone derivatives. The excited state multiplicity of the electronic states involved in the photoreaction were first explored. For this purpose, three samples of the same switch were irradiated simultaneously under different reaction conditions. Three solutions of **2c** in $CDCl_3$ (0.05 M) were prepared in Pyrex NMR tubes; the first was deoxygenated and used as reference, the second sample was saturated with O_2 (triplet quencher) by bubbling air for 15 min, and the third sample was deoxygenated and *cis*-piperilene (triplet quencher, 5 equiv.) was added. The three samples were simultaneously irradiated for 20 min with a 125 W medium-pressure Hg lamp. After irradiating, the ^{1}H NMR spectra of the samples were recorded to determine the isomer ratio at the given irradiation time. In all three cases, the isomer ratio was (80 ± 1)% *Z* and (20 ± 1)% *E*. Because the isomer ratio recorded after irradiating the samples for the same length of time were similar, it is plausible that the progress of the reaction took place through electronic states of singlet multiplicity, since the triplet quenchers had no effect on the outcome of the reaction. However, the photochemical product might be formed on a timescale that is too short for a quencher to intercept the excited state responsible for the photochemical transformation. In this case, the use of time-resolved spectroscopy could afford complementary data.

Theoretical Calculations

As discussed above, one of the key aspects of these photoswitches is their high thermal stability. Thus, we also performed a detailed computational study of the thermal reversion of the photoisomer. A deeper insight into this process is relevant to check the efficiency of the photoswitches in different applications as well as to allow for the rational design of new modifications. For this purpose, density functional theory (DFT) was used; a detailed description of the computational methods can be found in the Experimental Section.

We started our computational study by exploring the relative stability of the different isomers, including the steric and electronic factors introduced by the substituents R^1 and R^2 that could affect the thermal isomerization. We computed both isomers (*Z* and *E*) of several compounds to explore the effect of substitution. First, the effect of the methyl vs. the phenyl groups (substituent R^1) in the oxazolone ring was examined by computing the relative energies of isomers of **2h** and **2a** (see Figure 3). The change in substituent R^1 from methyl group to phenyl produces no significant variation in either the geometry or relative energy. All four compounds are planar and the bond lengths are very similar (only variations in the third decimal were found), including the C=N bond close to the modified substituent. Moreover, the energetics are essentially the same because their variations are below the theoretical threshold for the method used. Thus, from a thermal reactivity perspective, the inclusion of Ph or Me should provide similar results. However, the phenyl group should be relevant for

Table 3. Photostationary state for molecular photoswitches **2**.

Entry	R^1	R^2	Compd.	Ratio at PSS	
				% *Z*	% *E*
1	Ph	Ph	**2a**	75	25
2	Ph	*p*-MeOPh	**2c**	83	17
3	Ph	*o*-MeOPh	**2d**	65	35
4[a]	Ph	*p*-BrPh	**2e**	75	25
5	Me	Ph	**2h**	85	15
6	Me	*p*-Tol	**2i**	85	15
7	Me	*p*-MeOPh	**2j**	85	15
8	Me	*o*-MeOPh	**2k**	64	36
9[a]	Me	*p*-NO_2Ph	**2l**	83	17
10[a]	Me	*p*-CNPh	**2m**	75	25
11[a]	Me	*p*-$MeCO_2$Ph	**2n**	80	20
12[a]	Me	*p*-BrPh	**2o**	85	15
13	Me	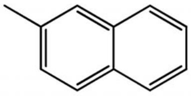	**2p**	83	17
14	Me	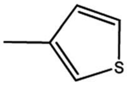	**2q**	60	40
15[a]	Me	*o*-Br	**2t**	60	40
16[a]	Ph	*p*-NO_2Ph	**2u**	80	20
17[a]	Ph	*p*-CN	**2v**	45	55

[a] Competing side reactions leading to partial photodecomposition were detected in the crude reaction mixture.

the photochemical reactivity because the extended conjugation leads to a redshift in the UV spectrum.

We next explored the effect of the electronic character of the substituent in the phenyl group of substituent R^2 by computing the energy-minimized structures of compounds **2v** and **2c**, in which either an electron-withdrawing (cyano) or electron-donating (methoxy) group is attached to the phenyl ring. The results obtained are shown in Figure S1. Again, the influence of the electronic character of the substituent in the phenyl group of substituent R^2 is limited. Only a slight variation in the central C=C bond length was found [1.358 Å in the cyano-substituted compound (**2v**) vs. 1.361 Å in the methoxy product (**2c**)]. The same bond has a length of 1.359 Å in the parent, unsubstituted product **2a**. This could be related to an increased energy barrier for thermal isomerization in the former compound, although the difference is very small. Finally, the effect of substitution in the *ortho* position in the phenyl group of substituent R^2 was explored by computing the energy-minimized structure of compound **2f** (Figure S2). In the case of *ortho*-substituted compounds, two different isomers can exist, each of them with two different conformers. For every central C=C configuration (*Z* and *E*), two different conformers are

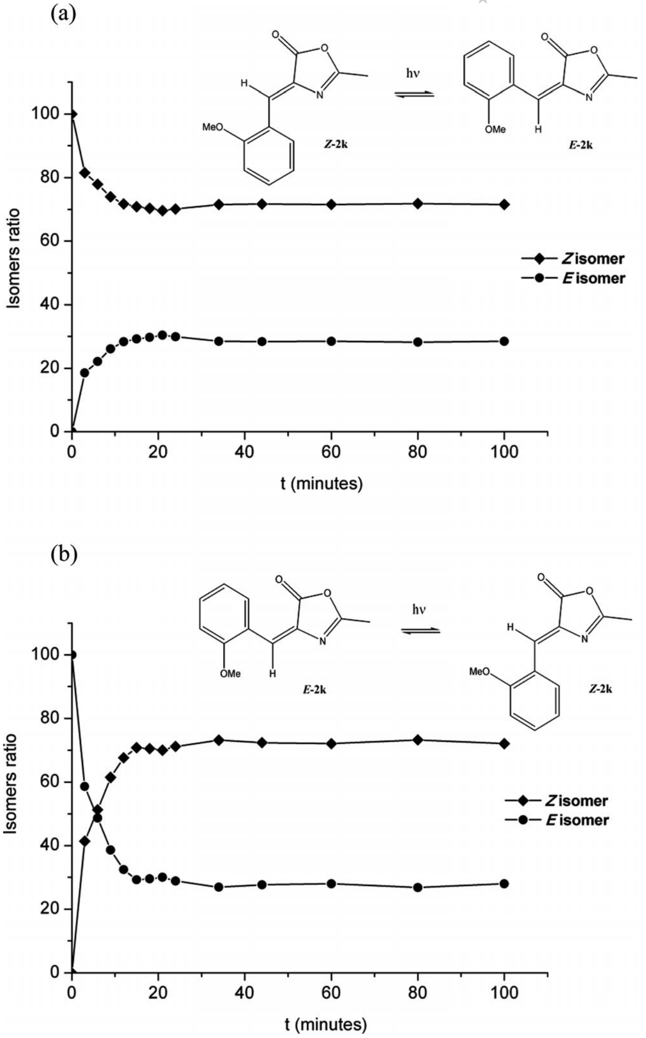

Figure 2. Isomer ratio vs. irradiation time starting from 100% *Z*-isomer (a), and 100% *E*-isomer (b) of compound **2k**.

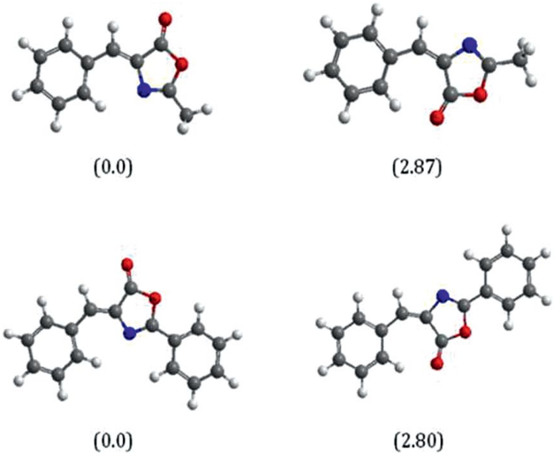

Figure 3. *Z* and *E* isomers and relative energies [kcal/mol] for compounds **2h** (top) and **2a** (bottom).

possible due to the orientation of the substituent in the aromatic ring. In this case, however, due to the size of the bromine atom, the two structures in which the Br atom is located near the oxazolone ring are clearly more unstable, presumably for steric reasons. This causes the molecule to move away from the planar disposition that is common to other compounds, especially when the Br atom is very close to the carbonyl moiety. Moreover, in the other two species with the Br atom located far from the oxazolone ring, a similar behavior is found in the relative stability of the *Z* and *E* isomers, the planar disposition of both molecules, and the central C=C distance (1.359 Å for the most stable isomer).

We also checked the feasibility of thermal isomerization. As shown above, only minor variations can be expected for the thermal reaction because the three types of structural modifications investigated experimentally had very limited effect on the energy and structure of the isomers. Thus, we explored the thermal isomerization path of **2a**, which has one of the simplest structures among this type of compound. The transition structure that connects both isomers is shown in Figure 4. This geometry is placed 61.9 kcal/mol higher in energy than the most stable isomer. The geometry features a twist of 87.5° between the rings that is consistent with the *E*/*Z* isomerization process together with a slight elongation of the central C=C bond (1.368 vs. 1.359 Å) in the most stable isomer, while the torsion angle between the vinylic hydrogen atom and the oxazolone ring is only 39°. Although the double bond character is maintained in this transition structure, the deformation of the geometry clearly points to a C=C isomerization, as shown by the pyramidalization of the C atom next to the aromatic ring and the dihedral angle between the rings. A frequency calculation on the transition structure allowed the transition vector to be obtained (Figure S3), with an imaginary frequency of 182.7 cm^{-1}. The main deformation associated with this vector is the hydrogen atom movement that connects the transition structure to the two valleys in the potential energy surface relative to the *E* and *Z* isomers.

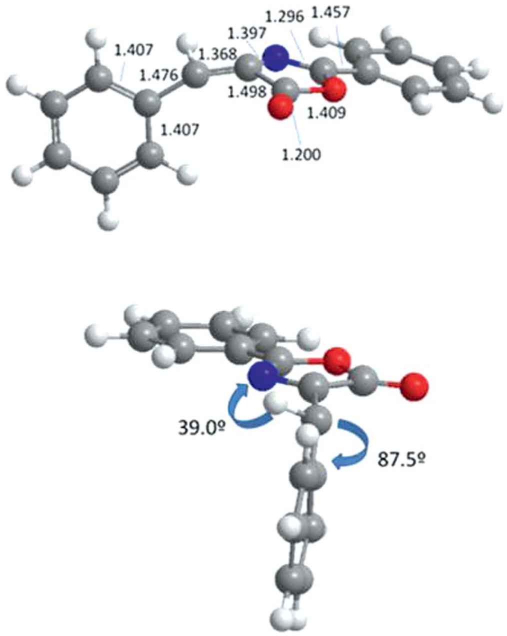

Figure 4. Transition structure for the ground-state isomerization of **2a**.

As a final step for the transition structure characterization, we performed an Intrinsic Reaction Coordinate (IRC) calculation; the results are shown in Figure 5.

As discussed above, only slight modifications are expected for compounds with variations of the structure. The high energy value computed for the transition structure is in agreement with the thermal stability found for this type of compound; these compounds were found to be stable to

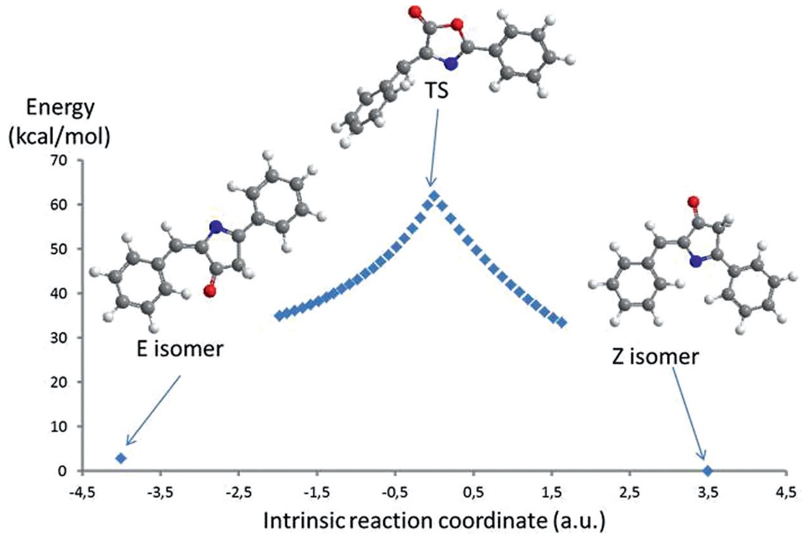

Figure 5. IRC starting from the computed transition structure of **2a**.

isomerization for days at room temperature, and isomerization was detected only after heating in toluene at 100 °C.

Conclusions

We have presented a comprehensive study of the synthesis and properties of a family of molecular photoswitches inspired by the GFP chromophore. These compounds show some features that make them promising candidates for use as light-activated switches in different applications. Oxazolone-based switches are easily synthesized in good yields and several functional groups can be incorporated within the basic structure. The choice of the substituents and solvents can be made on the basis of the projected application but also depending on the required photochemical features. The high thermal and photochemical stabilities should provide these switches with desirable fatigue resistance. The computational data allows an understanding of this key feature. The main drawback of oxazolones as photoswitches is the nucleophilic ring opening, and this issue should be solved before this type of compound could be used in biological applications. A detailed theoretical study of the photoprocesses could provide the necessary data for the design of improved versions of these photoswitches and also for tuning the switching properties to the requirements of specific applications. Future work on these systems will focus on the effect of light on these compounds once incorporated in complex systems.

Experimental Section

General Procedure for the Synthesis of Azalactones 2a–v: To a mixture of amino acid **1** with the appropriate substituent R^1 (1 equiv., 20 mmol) and sodium acetate (1 equiv., 20 mmol) in acetic anhydride (18.4 mL), was added the corresponding aldehyde with the required R^2 group (1 equiv., 20 mmol). The resulting mixture was stirred for 4 h at 100–110 °C, then stirred overnight at 25 °C. After this time, the target azalactone precipitated and was separated by filtration and washed with cold Et_2O (100 mL). The resulting solid was purified by flash chromatography on silica gel (hexanes/EtOAc, 2:1) to obtain the *Z*-isomer of **2a**–**v** in 60–90% yield.

Theoretical Calculations: The common hybrid functional B3LYP was used.[20] This is based on Becke's three parameter scheme consisting of the Slater exchange,[21] the exchange functional of Becke88,[22] and the HF exchange, as well as a mixture of the correlation functionals of Vosco–Wilk–Nusair[23] and Lee–Yang–Par.[24] The standard split-valence 6-31G* basis set[25] was employed. Geometry was fully optimized without any symmetry constraint for all model compounds. Optimized structures were characterized as minima or saddle points by frequency calculations, which also allowed the ZPE and thermal corrections with no scaling factors to be obtained. For transition structures, intrinsic reaction coordinates were also calculated at the same level of theory.[26] The Gaussian 03 program package[27] was used for all calculations.

Supporting Information (see footnote on the first page of this article): Synthesis, characterization data and copies of the ^1H and ^{13}C NMR spectra for switches **2**. Figures S1–S3. Cartesian coordinates for computed structures.

Acknowledgments

This research was supported by the Spanish Ministerio de Ciencia e Innovación (MICINN)/Fondos Europeos para el Desarrollo Regional (FEDER) (CTQ2011-24800). M. B.-L. thanks the Spanish Ministerio de Educación y Ciencia (MEC) for a grant.

[1] V. Balzani, A. Credi, M. Venturi, *Molecular Devices and Machines: Concepts and Perspectives for the Nanoworld*, Wiley-VCH Verlag, Germany, Weinheim, Germany, **2008**.
[2] C. Garcia-Iriepa, M. Marazzi, L. M. Frutos, D. Sampedro, *RSC Adv.* **2013**, *3*, 6241–6266.
[3] Y. Yokoyama, *Chem. Rev.* **2000**, *100*, 1717–1740.
[4] C. Yun, J. You, J. Kim, J. Huh, E. Kim, *J. Photochem. Photobiol. C: Photochem. Rev.* **2009**, *10*, 111–129.
[5] G. Berkovic, V. Krongauz, V. Weiss, *Chem. Rev.* **2000**, *100*, 1741–1754.
[6] B. L. Feringa, W. R. Browne, in: *Molecular Switches*, 2nd ed., Wiley-VCH, Weinheim, Germany, **2011**, p. 1–35.
[7] V. Balzani, A. Credi, M. Venturi, *Nano Today* **2007**, *2*, 18.
[8] a) G. Möller, M. Harke, H. Motschmann, D. Prescher, *Langmuir* **1998**, *14*, 4955–4957; b) H. Akiyama, K. Tamada, J. Nagasawa, K. Abe, T. Tamaki, *J. Phys. Chem. B* **2003**, *107*, 130–135.
[9] J. Ma, Y. Li, T. White, A. Urbas, Q. Li, *Chem. Commun.* **2010**, *46*, 3463–3465.
[10] M. Blanco-Lomas, S. Samanta, P. J. Campos, G. A. Woolley, D. Sampedro, *J. Am. Chem. Soc.* **2012**, *134*, 6960–6963.
[11] X-ray diffraction structures for oxazolone derivatives are available, see: a) M. Blanco-Lomas, P. J. Campos, D. Sampedro, *Org. Lett.* **2012**, *14*, 4334–4337; b) S. W. Ng, *Acta Crystallogr., Sect. E: Struct. Rep. Online* **2009**, *65*, o1857; c) K. Bowden, A. Perjéssy, J. Benko, W. Fabian, E. Kolehmainen, G. Melikian, O. Hritzov, K. Laihia, O. Vollárová, V. Taupuzian, N. Kiriakossian, M. Nissinen, *J. Chem. Res.* **2002**, 309.
[12] R. Heim, D. C. Prasher, R. Y. Tsien, *Proc. Natl. Acad. Sci. USA* **1994**, *91*, 12501–12504.
[13] a) S. Rafiq, B. K. Rajbongshi, N. N. Nair, P. Sen, G. Ramanathan, *J. Phys. Chem. A* **2011**, *115*, 13733–13742; b) V. Voliani, R. Bizzarri, R. Nifosì, S. Abbruzzetti, E. Grandi, C. Viappiani, F. Beltram, *J. Phys. Chem. B* **2008**, *112*, 10714–10722; c) J.-S. Yang, G.-J. Huang, Y.-H. Liu, S.-M. Peng, *Chem. Commun.* **2008**, 1344–1346.
[14] a) X. He, A. F. Bell, P. J. Tonge, *Org. Lett.* **2002**, *4*, 1523–1526; b) A. Kikuchi, E. Fukumura, S. Karasawa, H. Mizuno, A. Miyawaki, Y. Shiro, *Biochemistry* **2008**, *47*, 11573–11580.
[15] a) Y. L. N. Murthy, V. Christopher, U. V. Prasad, P. B. Bisht, D. V. Ramanaih, B. S. Kalanoor, S. A. Ali, *Synth. Met.* **2010**, *160*, 535–539; b) G. Ozturk, S. Alp, K. Ertekin, *Dyes Pigm.* **2007**, *72*, 150–156; c) G. Ozturk, S. Alp, S. Timur, *Dyes Pigm.* **2008**, *76*, 792–798.
[16] a) N. Baumann, M.-T. Sung, E. F. Ullman, *J. Am. Chem. Soc.* **1968**, *90*, 4157–4158; b) E. F. Ullman, N. Baumann, *J. Am. Chem. Soc.* **1970**, *92*, 5892–5899.
[17] J. E. Audia, J. J. Droste, J. S. Nissen, G. L. Murdoch, D. A. Evrard, *J. Org. Chem.* **1996**, *61*, 7937–7939.
[18] R. M. Herbst, D. Shemin, *Org. Synth.* **1939**, *19*, 1.
[19] Normalized parameters based on empiric data of solvent polarity (E_TN). For further information, see: C. Reichardt, *Solvents and solvent effects in organic chemistry*, 3rd ed., Wiley-VCH, Weinheim, Germany, **2003**, page 418.
[20] A. D. Becke, *J. Chem. Phys.* **1993**, *98*, 5648.
[21] J. C. Slater, *Quantum Theory of Molecules and Solids*, vol. 4: *The Self-Consistent Field for Molecules and Solids*, McGraw Hill, New York, **1974**.
[22] A. D. Becke, *Phys. Rev. B* **1988**, *38*, 3098.
[23] S. H. Vosco, L. Wilk, M. Nusair, *Can. J. Phys.* **1980**, *58*, 1200.
[24] C. Lee, W. Yang, R. G. Parr, *Phys. Rev. B* **1988**, *37*, 785.

[25] P. C. Hariharan, J. A. Pople, *Theor. Chim. Acta* **1973**, *28*, 213–222.

[26] a) C. Gonzalez, H. B. Schlegel, *J. Chem. Phys.* **1990**, *94*, 5523; b) C. Gonzalez, H. B. Schlegel, *J. Chem. Phys.* **1989**, *90*, 2154.

[27] M. J. Frisch, G. W. Trucks, H. B. Schlegel, G. E. Scuseria, M. A. Robb, J. R. Cheeseman, J. A. Montgomery Jr, T. Vreven, K. N. Kudin, J. C. Burant, J. M. Millam, S. S. Iyengar, J. Tomasi, V. Barone, B. Mennucci, M. Cossi, G. Scalmani, N. Rega, G. A. Petersson, H. Nakatsuji, M. Hada, M. Ehara, K. Toyota, R. Fukuda, J. Hasegawa, M. Ishida, T. Nakajima, Y. Honda, O. Kitao, H. Nakai, M. Klene, X. Li, J. E. Knox, H. P. Hratchian, J. B. Cross, C. Adamo, J. Jaramillo, R. Gomperts, R. E. Stratmann, O. Yazyev, A. J. Austin, R. Cammi, C. Pomelli, J. W. Ochterski, P. Y. Ayala, K. Morokuma, G. A. Voth, P. Salvador, J. J. Dannenberg, V. G. Zakrzewski, S. Dapprich, A. D. Daniels, M. C. Strain, O. Farkas, D. K. Malick, A. D. Rabuck, K. Raghavachari, J. B. Foresman, J. V. Ortiz, Q. Cui, A. G. Baboul, S. Clifford, J. Cioslowski, B. B. Stefanov, G. Liu, A. Liashenko, P. Piskorz, I. Komaromi, R. L. Martin, D. J. Fox, T. Keith, M. A. Al-Laham, C. Y. Peng, A. Nanayakkara, M. Challacombe, P. M. W. Gill, B. Johnson, W. Chen, M. W. Wong, C. Gonzalez, J. A. Pople, *Gaussian 03*, revision C.02, Gaussian, Inc., Wallingford CT, **2004**.

Received: May 2, 2013

Molecular Devices

A family of photoswitches is comprehensively studied. These compounds are easily synthesized and show interesting features for their use in a number of applications. They are thermally and photochemically stable, and the photostationary state can be tuned by the substituents, solvent and irradiation conditions.

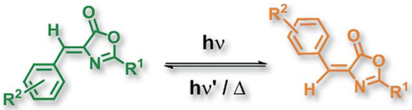

M. Blanco-Lomas, I. Funes-Ardoiz, P. J. Campos, D. Sampedro* 1–9

Oxazolone-Based Photoswitches: Synthesis and Properties

Keywords: Photochemistry / Molecular devices / Photoswitches / Density functional calculations / Heterocycles